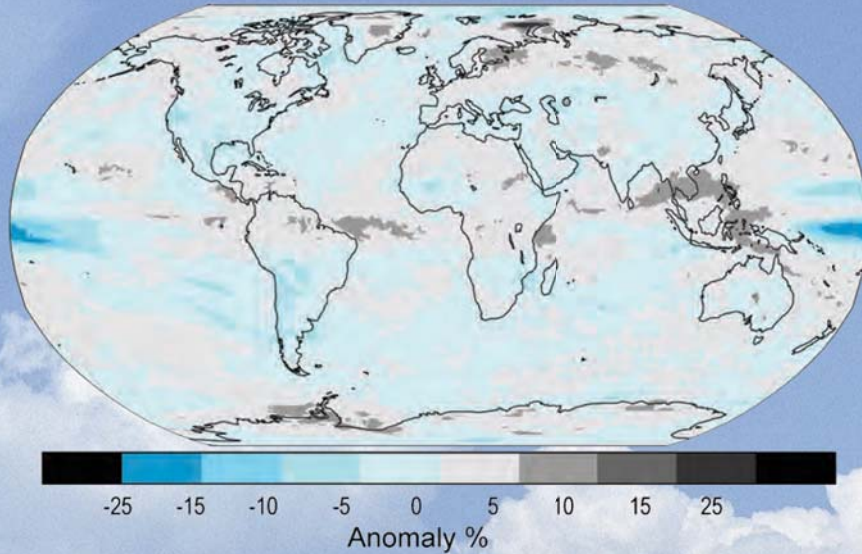


STATE OF THE CLIMATE IN 2008

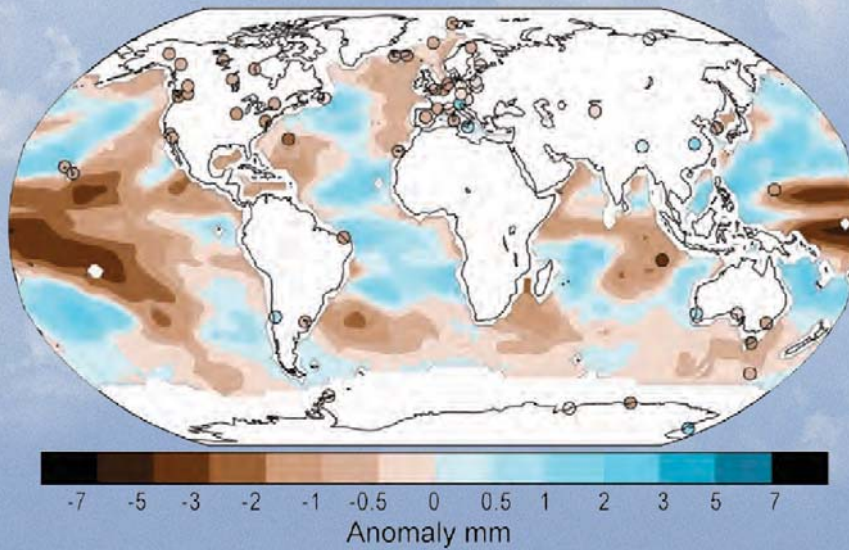
T. C. PETERSON AND M. O. BARINGER, Eds.

ASSOCIATE Eds.: H. J. DIAMOND, R. L. FOGT, J. M. LEVY, J. RICHTER-MENGE,
P. W. THORNE, L. A. VINCENT, AND A. B. WATKINS

Cloud cover



Total column water vapor



Special Supplement to the *Bulletin of the American Meteorological Society*
Vol. 90, No. 8, August 2009



that also hold in 2005 through 2007 (not shown). The regions around the subtropical salinity maxima are mostly salty with respect to WOA 2001. Most of the high-latitude climatologically fresh regions appear fresher than WOA 2001, including most of the ACC near 50°S and the subpolar gyre of the North Pacific. These patterns may be consistent with an increase in the hydrological cycle (i.e., more evaporation in drier locations and more precipitation in rainy areas), as seen in simulations of global warming. These simulations suggest this signal might be discernible over the last two decades of the twentieth century (Held and Soden 2006), consistent with the multiyear nature of these anomalies. In addition, a study of global subsurface salinity anomalies comparing 2000 Argo data to those from the 1990 World Ocean Circulation Experiment and prior historical data suggests that these patterns are persistent and decadal (K. P. Helm et al. 2009, manuscript submitted to *Nature Geosci.*).

Nonetheless, there may be alternate explanations. It is possible that the climatology, being based on relatively sparse data distributions in many parts of the oceans, may tend to underestimate regional extrema that the well-sampled Argo array can better resolve, or that the climatology contains regional biases on seasonal or longer time scales that are not present in the Argo data. Also, some of these patterns might be explained by interannual variability in large-scale oceanic currents or atmospheric features such as the ITCZs.

For example, in contrast to the other high-latitude areas, the subpolar North Atlantic and Nordic Seas in 2008 are anomalously salty with respect to WOA 2001 (Fig. 3.13a), as they have been since at least 2005 (not shown). This salty subpolar anomaly is inconsistent with a simple increase in the strength of the hydrological cycle. However, the pattern may have less to do with local evaporation and precipitation fields than with northward spread of saltier waters from the south. The salty anomaly in this region is consistent with a stronger influence of subtropical gyre waters in the northeastern North Atlantic in recent years and a reduced extent of the subpolar gyre (Hátún et al. 2005).

Salinity in the tropics exhibits strong interannual variability due to influences of phenomena such as the ENSO cycle (e. g., Ando and McPhaden 1997). For instance, the ITCZ in the central and eastern tropical Pacific is anomalously salty in 2008 (Fig. 3.13a), with some of that anomaly due to changes since 2007 (Fig. 3.13b), probably caused by an ongoing La Niña in 2008 reducing atmospheric convection and thus changing patterns of evaporation (Fig. 3.8) and precip-

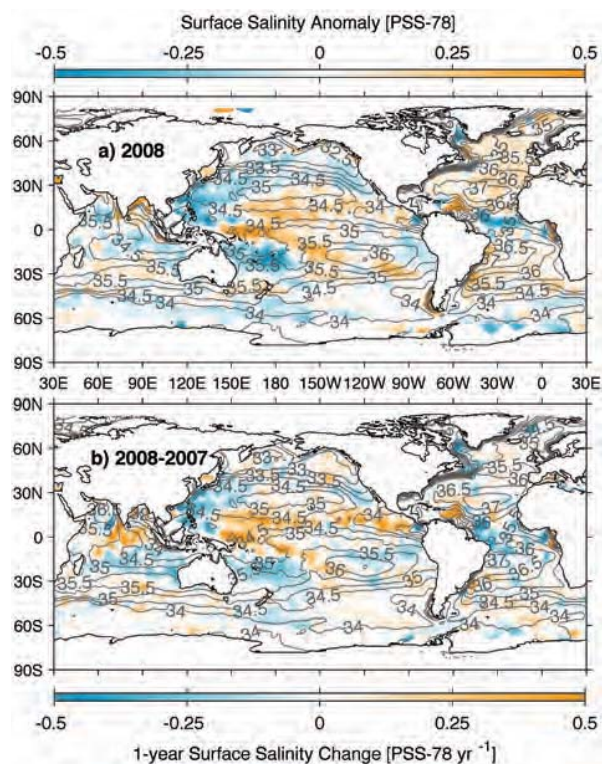


FIG. 3.13. (a) Map of the 2008 annual surface salinity anomaly estimated from Argo data (colors in PSS-78) with respect to a climatological salinity field from WOA 2001 (gray contours at 0.5 PSS-78 intervals). (b) The difference of 2008 and 2007 surface salinity maps estimated from Argo data [colors in PSS-78 yr⁻¹ to allow direct comparison with (a)]. White areas are either neutral with respect to salinity anomaly or too data poor to map. While salinity is often reported in PSU, it is actually a dimensionless quantity reported on the PSS-78.

itation in the region. In contrast, freshening in the far western tropical Pacific is evident, as is freshening in the Atlantic ITCZ. In addition, a strong fresh anomaly south of India in the tropics in 2007 (not shown) is absent in 2008 (Fig. 3.13a), again due to changes taking place over a 1-yr interval (Fig. 3.13b).

g. Surface current observations—R. Lumpkin, G. Goni, and K. Dohan

Near-surface currents are measured in situ by drogued¹ satellite-tracked drifting buoys and by current meters on moored ATLAS buoys. (Drifter

¹ A drogued buoy is attached to a large cylindrical canvas sea anchor. The drogue (sea anchor) dominates the surface area of the drifter and ensures that it follows currents at the drogue depth of 15 m rather than being blown by the wind.

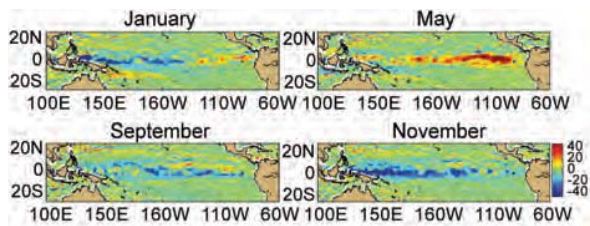


FIG. 3.14. OSCAR monthly averaged zonal current anomalies (cm s^{-1}), positive eastward, with respect to seasonal climatology for Jan, May, Sep, and Nov 2008.

data are distributed by NOAA/AOML at www.aoml.noaa.gov/phod/dac/gdp.html. Moored data are distributed by NOAA/PMEL at www.pmel.noaa.gov/tao. OSCAR gridded currents are available at www.oscar.noaa.gov/. AVISO gridded altimetry is produced by SSALTO/DUACS and distributed with support from CNES, at www.aviso.oceanobs.com/) During 2008, the drifter array ranged in size from a minimum of 918 drogued buoys to a maximum of 1,065, with a median size of 966 drogued buoys (undrogued drifters continue to measure SST but are subject to significant wind slippage; Niiler et al. 1987). The moored array included 35 buoys with current meters, all but two between 10°S and 21°N . Tropical moorings are maintained by the Pacific Ocean TAO, Atlantic Ocean PIRATA, and Indian Ocean RAMA projects. The two nontropical moored current meter sites of the Global Ocean Observing System are the Kuroshio Extension Observatory (32°N , 145°E) and Ocean Station Papa (50°N , 145°W).

Satellite-based estimates of ocean currents are produced by NOAA's OSCAR project, which uses satellite altimetry, winds, and SST to create 1° resolution surface current maps for the 0–30-m layer of the ocean (Bonjean and Lagerloef 2002). Anomalies are calculated with respect to the time period 1992–2002.

1) SURFACE CURRENT ANOMALIES IN 2008

The instantaneous distribution of current anomalies from the 1992–2002 mean mainly reflects the distribution of eddy kinetic energy associated with mesoscale eddies (cf., Stammer 1998; Lumpkin and Pazos 2007). To be significant, we require that anomalies must exceed the mean standard deviation (square root of eddy kinetic energy) with a distribution extending over several Eulerian length scales (Stammer 1998). By this definition, the only significant short-term (seasonal

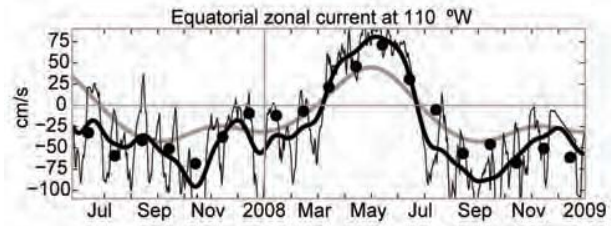


FIG. 3.15. Daily (thin black) and 15-day low-passed (thick black) zonal currents (positive eastward) measured at the equatorial TAO mooring at 110°W , at a depth of 10 m. Also shown are the mean seasonal cycle (gray) and OSCAR monthly mean zonal currents (black dots) at this location.

to annual) anomalies in 2008 occurred in the tropical Pacific Ocean. Longer-term variations can be resolved elsewhere and are discussed in the next section.

In the equatorial Pacific, the year began with large westward current anomalies in the western basin, associated with strong La Niña conditions, extending to 140°W (Fig. 3.14). In the eastern basin, weak eastward anomalies were seen from 120°W to the South American coast. These eastward anomalies grew in intensity and spatial coverage despite enhanced easterly surface winds (Fig. 4.4) At 110°W , this eastward anomaly pattern peaked in early May (Fig. 3.15), when the seasonal cycle typically reaches its maximum eastward speed. The eastward anomalies were $20\text{--}40 \text{ cm s}^{-1}$ above typical May values and extended from South America to 160°E (Fig. 3.14). These anomalies deepened the thermocline in the eastern equatorial Pacific (Fig. 4.3),

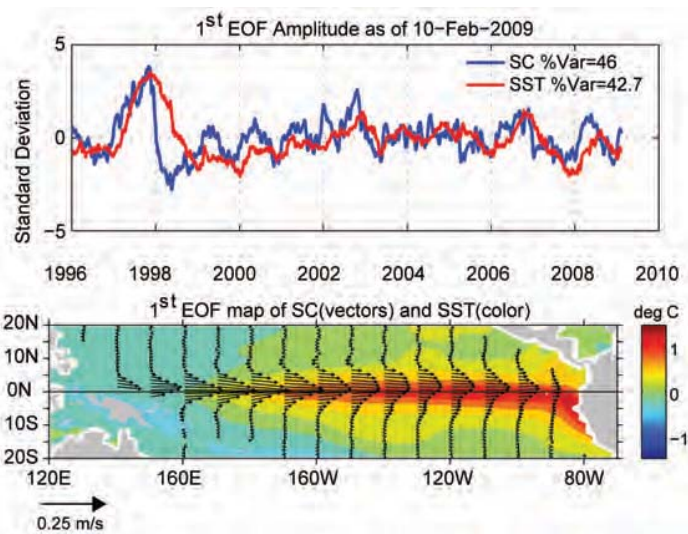


FIG. 3.16. Principal EOF of surface current (“SC”) and SST anomaly variations in the tropical Pacific. (top) Amplitude time series of the EOFs normalized by their respective std devs. (bottom) Spatial structures of the EOFs.

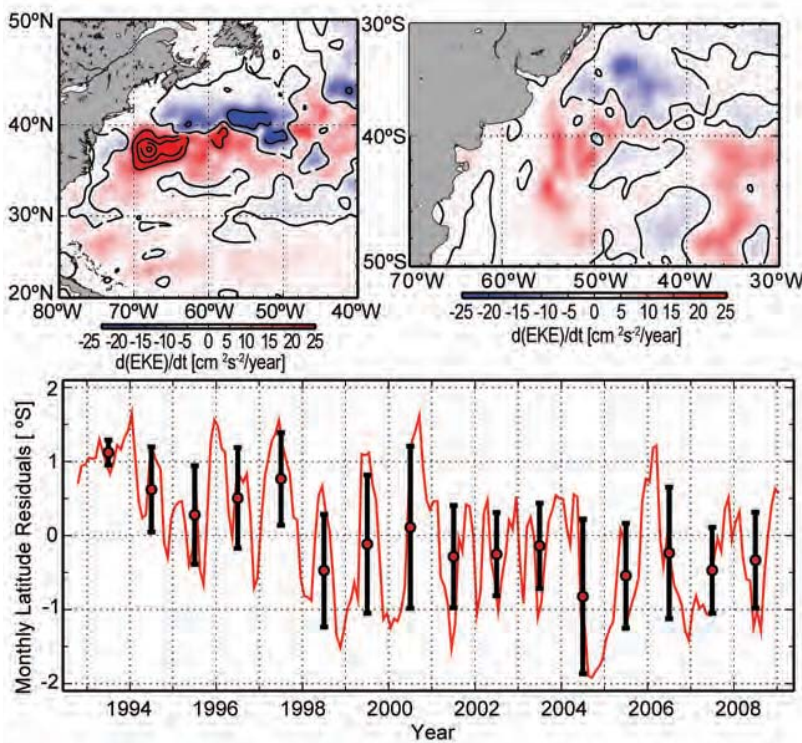


FIG. 3.17. Trends in geostrophic EKE for 1993–2008 in (top left) the Gulf Stream region and (top right) the Brazil–Malvinas Confluence, calculated from satellite altimetry. (bottom) Location of the Brazil Current separation with respect to its mean position over the period 1993–2008. Circles with bars indicate annual means and 2 std devs of the values in each calendar year.

increasing upper-ocean heat content and resulting in warm SST anomalies (Fig. 4.2). Warm SSTs were concentrated west of 120°W on the equator in May, when the Niño-3.4 index (which had been negative from January–April) became neutral (Fig. 4.1).

This El Niño–like surface current pattern, associated with the transition from La Niña to ENSO-neutral conditions, weakened in early boreal summer and had disappeared by early fall when warm SST anomalies in the eastern equatorial Pacific peaked and the monthly averaged Niño-3 and Niño-3.4 indices reached their maximum 2008 value (Fig. 4.1).

Through midboreal summer, westward current anomalies developed in the eastern part of the Pacific basin, reaching a peak of 40 cm s⁻¹ (with respect to seasonal climatology) in September at 110°W (Fig. 3.15; anomaly is difference between the black and gray curves). This pattern spread westward in late 2008, reaching the western Pacific with maximum anomalies of 65–75 cm s⁻¹ in November (Fig. 3.14). The resulting shallower thermoclines in the eastern Pacific were associated with cool SST anomalies and decreases in the Niño-3 and Niño-3.4 indices over

the period October–December (Fig. 4.1).

Surface current anomalies in the equatorial Pacific typically lead SST anomalies by several months, with a magnitude that scales with the SST anomaly magnitude. Recovery to normal current conditions is also typically seen before SST returns to normal. Thus, current anomalies in this region are a valuable predictor for the evolution of SST anomalies and their related climate impacts. This leading nature can be seen clearly in the first principal EOF of surface current anomaly and separately of the SST anomaly in the tropical Pacific basin (Fig. 3.16), extending back to 1996.

2) LONG-TERM CHANGES IN SURFACE CURRENTS

Geostrophic EKE can be derived from gridded AVISO altimetry fields and reveals long-term trends in the Atlantic Ocean over the period 1993–2008 that may indicate a change of intensity and

location of major surface currents. Along the axis of the Gulf Stream (Fig. 3.17) an increase in EKE to the south and a decrease to the north may indicate a long-term shift to the south in the current. In the southwestern Atlantic, a similar situation occurs, where the linear trend of EKE exhibits negative (positive) values to the north (south) of 38°S in the Brazil–Malvinas Confluence region. As with the Gulf Stream, this linear trend may indicate a shift in the surface current field to the south. Altimetry observations (bottom, Fig. 3.17) also show that the separation of the Brazil Current from the continental shelf break (Goni and Wainer 2001) has shifted south over the period 1993–2008. However, since 2004 (when the Brazil Current reached its southernmost separation point) it has tended to shift to the north.

h. The meridional overturning circulation—M. O. Baringer, C. S. Meinen, G. C. Johnson, T. O. Kanzow, S. A. Cunningham, W. E. Johns, L. M. Beal, J. J.-M. Hirschi, D. Rayner, H. R. Longworth, H. L. Bryden, and J. Marotzke

The meridional redistribution of mass and heat associated with the large-scale vertical circulation with-